ELSEVIER

Journal of Structural Geology 29 (2007) 898–912

JOURNAL OF STRUCTURAL GEOLOGY

www.elsevier.com/locate/jsg

Fracture pattern of Thjórsárdalur central volcano with respect to rift-jump and a migrating transform zone in South Iceland

Maryam Khodayar*, Hjalti Franzson

Iceland GeoSurvey (Íslenskar orkurannsóknir), Grensásvegur 9, 108 Reykjavík, Iceland

Received 12 August 2005; received in revised form 27 November 2006; accepted 28 November 2006
Available online 1 February 2007

Abstract

An analysis of dykes, mineral veins, and tectonic joints in the Matuyama-age Thjórsárdalur volcano provides insights into the relative development of rift and transform zones at slow-spreading centres. Rifting resulted in the formation of NNE fractures. Transform faulting gave rise to shear fractures striking predominantly N–S and ENE, parallel to the main earthquake fractures of the South Iceland Seismic Zone (SISZ), but also WNW, E–W, and NNW. All fractures were filled with the same geothermal fluid and magma. The strikes, motions, and fracture cross-cuttings show that the transform fault was active early in the history of the volcano, coeval with the rift(s). The shear fractures are consistent with a Riedel shear model of an E–W transform zone, and with a minimum principal stress, σ_3, striking N135°E to N150°E. These values are close to the direction of extension across the Eastern Rift Zone (ERZ), supporting an interpretation that the E–W shear zone has migrated from the latitude of Thjórsárdalur to the SISZ with the southward propagation of the ERZ. Migration of synchronous transform and rift systems at a slow-spreading centre yields a distinctive fracture pattern, but lacks some of the elements found at similar migration sites for fast-spreading centres.

Keywords: Thjórsárdalur central volcano; South Iceland Seismic Zone; Rift-jump; Migrating transform zone; Iceland Hotspot; Hengill

1. Introduction

Tectonic plate boundaries are known to become unstable, especially near hotspots where the crust drifts over areas of high volcanic production. When divergent plate boundaries shift, one rift segment propagates (gains in its active length) while the other one recedes (loses in its active length), and the transform fault connecting them migrates to accommodate the geometric and kinematics for these rift segments. In the process, blocks of crust (rift-jump blocks) caught between the receding and the propagating rifts may be transferred from one plate to the other. These behaviours are observed in both slow-spreading (Jóhannesson, 1980; Helgason, 1984; Einarsson, 1991; Kristjánsson and Jónsson, 1998; Khodayar and Einarsson, 2002a) and fast-spreading rift zones (Shih and Molnar, 1975; Hey et al., 1980; Kleinrock and Hey, 1989; Phipps Morgan and Kleinrock, 1991). The tectonics of these shifts is better understood for fast-spreading zones than slow-spreading ones. Our paper aims to offer new insights into these behaviours at slow-spreading zones with a case study from Iceland.

Several active and extinct rifts and transform zones run through Iceland (Fig. 1). The rift segments show evidence of jumps (relocation) going back at least 15 Ma (Jónsson et al., 1991; Jancin et al., 1985). These jumps have occurred either every 1–2 m.y., with the active segments shifting about 20–40 km away from their initial positions, or every 6–8 m.y. with relocations of the order of 100–200 km (Helgason, 1984). One of these jumps, from the Snæfellsnes Rift Zone (SRZ, 15–6 Ma) to the Reykjanes-Langjökull Rift Zone (RLRZ, 6 Ma–present), occurred about 6–7 Ma (Jóhannesson, 1980). A Tertiary transform zone may have connected these

* Corresponding author. Tel.: +354 528 1522; fax: +354 528 1699.
E-mail address: mak@isor.is (M. Khodayar).

0191-8141/$ - see front matter © 2007 Elsevier Ltd. All rights reserved.
doi:10.1016/j.jsg.2006.11.007

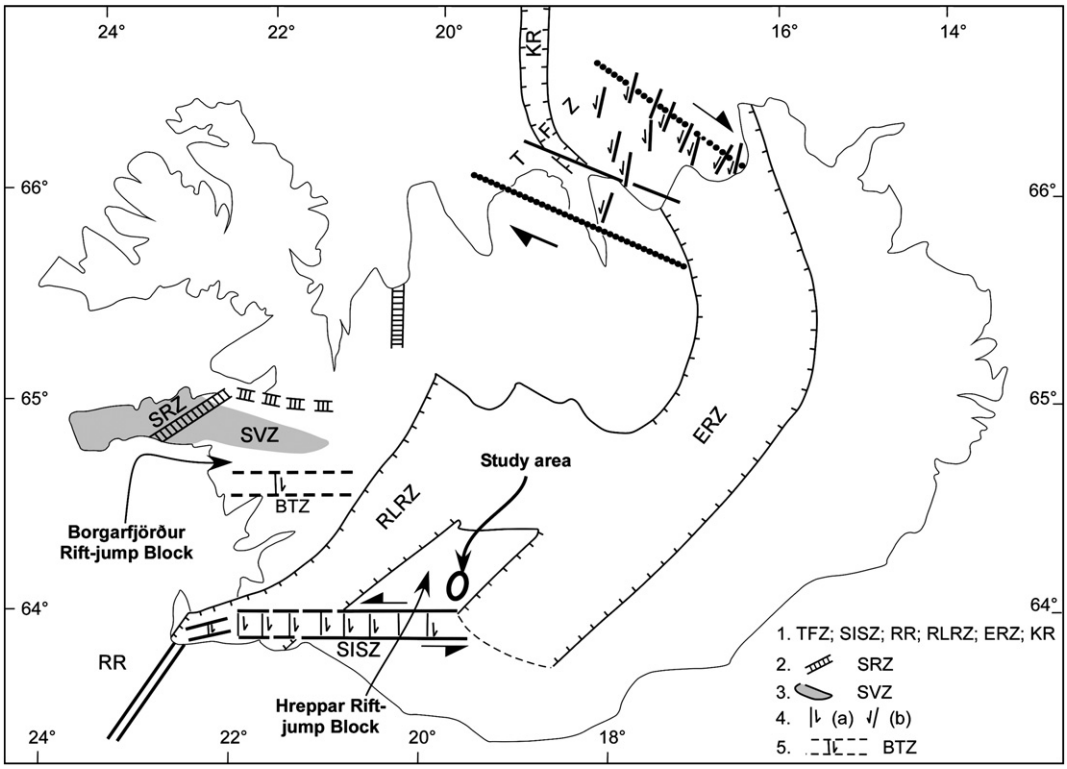

Fig. 1. Major tectonic elements in Iceland (modified from Khodayar and Einarsson, 2002a) and location of the study area. 1. TFZ: Tjörnes Fracture Zone; SISZ: South Iceland Seismic Zone (note that only the strike of the main earthquake fractures are shown within the SISZ); RR: Reykjanes Ridge; RLRZ: Reykjanes-Langjökull Rift Zone; ERZ: Eastern Rift Zone; KR: Kolbeinsey Ridge. 2. SRZ: Snæfellsnes Rift Zone (extinct Tertiary rift). 3. SVZ: Snæfellsnes Volcanic Zone. 4. (a) Dextral strike-slip fault; (b) sinistral strike-slip fault. 5. BTZ: Borgarfjörður Transform Zone.

segments around 65°N (Sigurðsson, 1970; Jancin et al., 1985) and probably as far south as 64°40′N (Khodayar and Einarsson, 2002a). The ages of the lavas in the Eastern Rift Zone (ERZ) (Jóhannesson and Sæmundsson, 1998) indicate that another jump of the rift, from the RLRZ to the southern half of the ERZ, began about 2–3 Ma. The active transform zone of the South Iceland Seismic Zone (SISZ) connects these segments. No transform zone connects the northern part of the RLRZ and the ERZ around 65°N at the present time. For this reason, Einarsson (1991) proposed that the SISZ may have migrated southward.

Icelandic rifts develop central volcanoes and extensional fissure swarms (Walker, 1963; Sæmundsson, 1978) with fractures striking parallel to the zones, e.g. NNE to NE south of 65°N (Jóhannesson and Sæmundsson, 1998). Transform zones develop essentially conjugate sets of strike-slip faults, striking N–S and ENE south of 65°N, as well as bookshelf tectonics (Einarsson et al., 1981, 2005; Sigmundsson et al., 1995). The tectonic patterns of both rift and transform zones have been separately studied in detail. The interaction between rift and transform zones, particularly during a relocation (jump) of the slow-spreading centre is not well documented.

We investigate this interaction in this paper by analysing the dykes, mineral veins, and joints of the southern part of the Thjórsárdalur central volcano in the Hreppar rift-jump block, which is bounded by the SISZ, the ERZ, and the RLRZ (Figs. 1–3). First, we demonstrate that the fracture pattern of Thjórsárdalur consists of six sets. One of these sets is rift-parallel, but the other five are mostly composed of shear fractures. A similar fracture pattern is seen in the Hreppar block (Khodayar and Einarsson, 2002b; Khodayar and Franzson, 2004), but this is the first time we observe it within a central volcano. Secondly, we report the fracture pattern of the SISZ and apply the Riedel shear model to interpret the secondary fractures in both the SISZ and an older transform zone at the latitude of Thjórsárdalur volcano for comparison. We propose a coeval rift and transform fault-system development in Thjórsárdalur that applies to other volcanoes, such as Hengill and Hekla (Fig. 2a). Thus, the analysis has applicability to the interaction of rift and transform zones at slow-spreading centres. Also, the results have implications for geothermal activity and natural hazards in Iceland.

2. Geological setting

The Hreppar Formation in South Iceland consists of late Tertiary to Pleistocene basalts, hyaloclastites, sediments, and minor acidic intrusions. The Formation ranges in age from 3.1 m.y. to 0.7 m.y. (Aronson and Sæmundsson, 1975). Acidic rocks are found within the Stóra-Laxá and the Thjórsárdalur central volcanoes (Figs. 1 and 2a). Sills are common in the volcanic succession and contribute to the build-up of the crust (Khodayar and Einarsson, 2002b; Khodayar and Franzson, 2004). Interglacial columnar-jointed lavas younger than

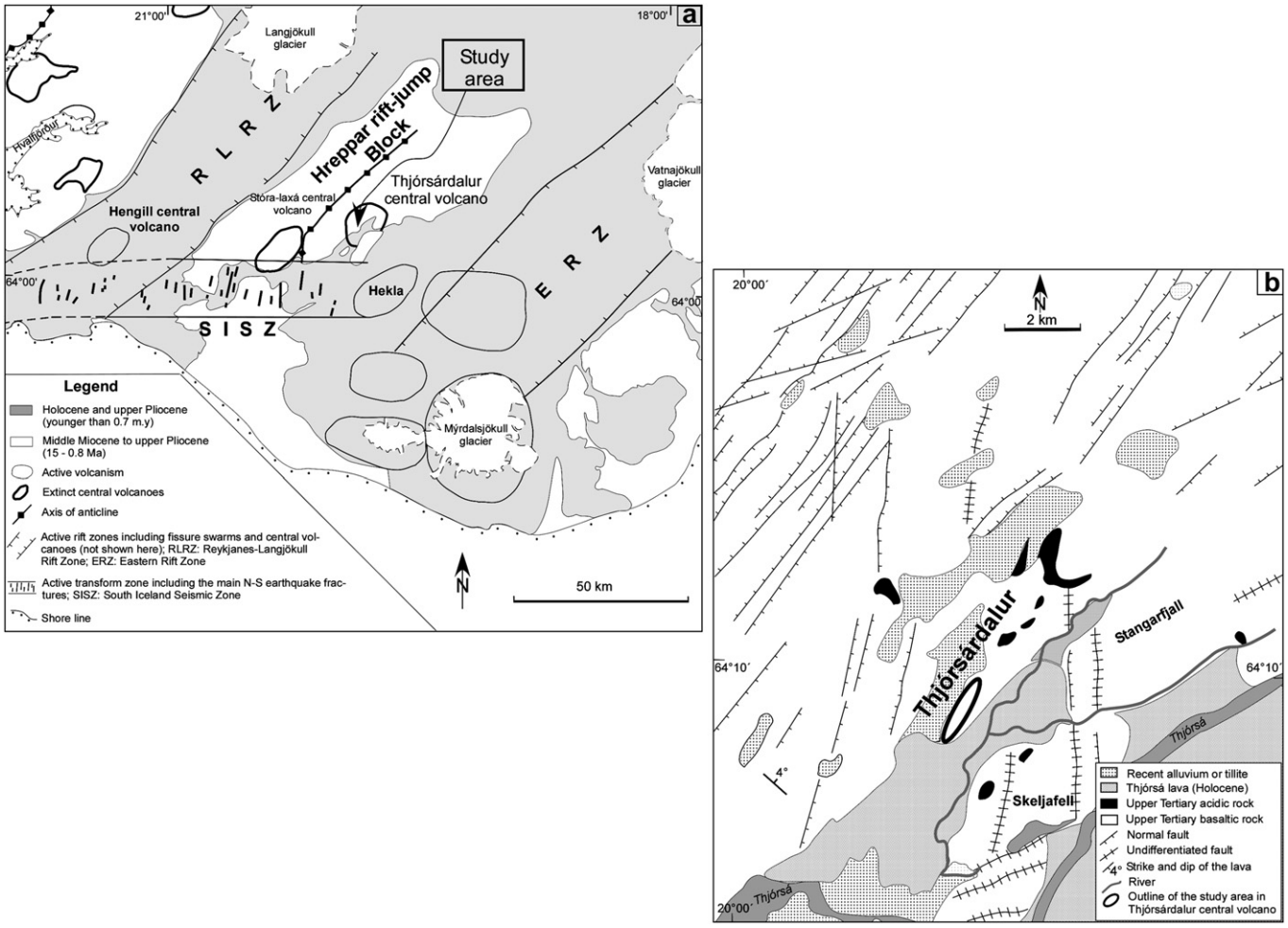

Fig. 2. (a) Geological map of the southern part of Iceland. Only the main N–S earthquake fractures are shown within the SISZ (see text for explanation). (b) Simplified geological map of Thjórsárdalur and vicinity. Both maps are modified from Jóhannesson and Sæmundsson (1998).

0.7 m.y. (Sæmundsson, 1970) and the 8000-yr-old Thjórsá lava (Hjartarson, 1988) cover the Hreppar Formation in places (Fig. 2a,b). The Hreppar Formation is presently eroded down to a paleoburial depth of 500–700 m (Sæmundsson, 1970).

Previous tectonic studies have already revealed normal faults striking NNE, ENE and N–S in the Hreppar block (Fig. 2b). Faults striking NW, E–W, and WNW are also common, and so are dykes, mineral veins, and joints along all the six strikes (Khodayar and Einarsson, 2002b; Khodayar and Franzson, 2004). A fraction of the faults displays oblique-slip striae with a pitch of 30–60°. The majority of the non-rift-parallel faults, however, shows both dip- and strike-slips, with few cross-cutting striae to reveal the chronology of the fault types (Khodayar and Einarsson, 2002b; Khodayar and Franzson, 2004). Some N–S faults in the Hreppar block can be traced into the SISZ (Khodayar and Einarsson, 2002b), where they are seismically active dextral strike-slip faults (Einarsson et al., 1981) (Figs. 1 and 2a), and form a conjugate set with the shorter ENE sinistral earthquake faults (Einarsson et al., 2005).

The Thjórsárdalur central volcano is considered to be of Matuyama age, starting around 2 Ma (Friðleifsson et al., 1980; Vilmundardóttir et al., 1983; Jónsson et al., 1991; Kristjánsson et al., 1998) and ceasing around 1–0.7 Ma (Kristjánsson et al., 1998), before being eroded and partially covered by interglacial lavas. The lifetime of the Thjórsárdalur volcano may have been as long as 1 m.y., similar to that of many other Icelandic central volcanoes. The total thickness of the strata in the volcano is unknown, but the present surface corresponds to a paleoburial depth of 500–700 m, implying that the tectonic history discussed here is contemporaneous with or younger than the exposures studied. The study area is about 12 km north of the active transform zone of the SISZ. The host rock of the measured dykes, mineral veins, and joints consists of homogeneous volcanic tuff, which is glacially smoothed and gives an exceptional map view of the structures.

3. Structural analysis

We focused on five outcrops spread over a distance of 3.4 km (Figs. 3a,b and 4a). We measured the strike and thickness of dykes and mineral veins, and the strike of tectonic joints. In the absence of absolute dating of the fractures, only a relative chronology of the fracture relationship and

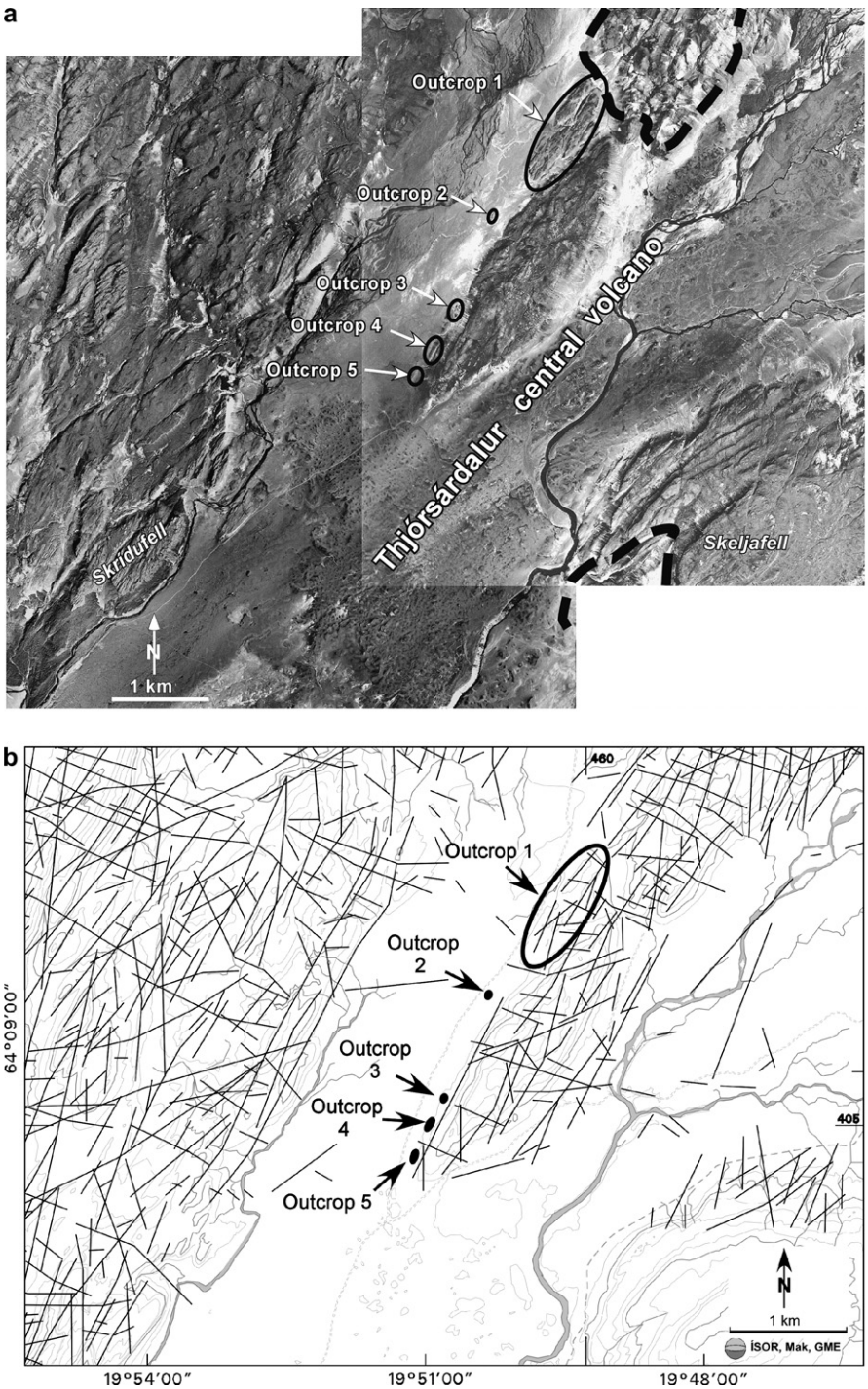

Fig. 3. (a) Aerial photograph of Thjórsárdalur central volcano (© *Landmælingar Íslands, licence L05070008*). The white arrows show the locations of the outcrops studied. Broken black lines show the areas of exposure of acidic rocks on the surface. (b) Our interpretation of the undifferentiated major fractures (faults and dykes) observed on aerial photographs of (a).

secondary mineralisation was defined. The dip of most veins could not be measured due to their position at the surface of the tuffs. The few veins with visible dip are similar to the thousands of veins measured in the immediate vicinity of Thjórsardalur in the Hreppar Formation (Khodayar and Einarsson, 2002b; Khodayar and Franzson, 2004), which are mostly steeply dipping, although a few have moderate dip.

Most measurements are from outcrop 1, which is the largest of the five (Fig. 3). In our analysis, we treated the five data sets both separately (Fig. 4a), and as a whole (Fig. 4b) because the structures are in similar rock type and age with no major spatial tectonic change between outcrops.

In the following, we shall write N–S, NNE, etc. to denote the strike-ranges of the fractures. These are, from 0° to 180°E,

as follows: N–S (N171°E–N20°E); NNE–NE (N21°E–N50°E); ENE (N51°E–80°E); E–W (N81°E–N100°E); WNW (N101°E–N140°E); and NNW (N141°E–N170°E).

3.1. Dykes, mineral veins, and joints

A total of 33 dyke segments were measured in four outcrops (Figs. 4a,b and 5a). Except for two rhyolitic dykes, they are tholeiitic aphyric or with plagioclase and pyroxene phenocrysts, but rarely with olivine. The trace length of the dykes ranges from 18 to 110 m and their thickness from 0.10 to 1.4 m, reaching 2 m in one case. The thickest dykes are in outcrop 1. One dyke is a pillow dyke (Fig. 5b) and shows radial fracturing (Fig. 5c). The dyke strikes dominantly WNW with a bend to the NE (Fig. 5b,c), undulating along the strike (Fig. 5a,b). Non-pillow dykes show a variety of geometries such as smoothly varying strike orientations (Fig. 5a), bifurcation (Fig. 5c), especially at their tips (Fig. 5d), and non-overlapping segmentation (Fig. 5e). Some of these dyke geometries are similar to those of blunt-ended dyke segments (Kattenhorn and Watkeys, 1995).

We measured 596 mineral veins in five outcrops (Fig. 4). The veins are filled with calcite and zeolites, or less frequently with clay and opal. Clay alteration of the wall rock, up to 20 cm thick, is often observed along veins. The veins vary in length from 20 cm to several metres (Fig. 6). The vein network (Fig. 6a,b) is especially intense in the eastern half of outcrop 1 (Fig. 5a). The veins are generally less than 1 cm thick but may occasionally reach 4 cm. Outside of the zone of intense mineralisation, up to 7 cm thick veins are observed filled with aragonite only.

A total of 324 joints were measured in five outcrops (Fig. 4a). We consider these structures to be tectonic joints because they were found in the hyaloclastite tuffs, and not in lavas, where they might have been confused with cooling joints. The length of the joints ranges from one to several metres at the surface of the tuffs. All joints show dilational character of the order of several millimetres. Often they crop out as a single prominent fracture, but sometimes shorter joints lie locally parallel to the main joints. Field evidence did not reveal whether later shearing occurred along the joints.

4. Relative chronology and fracture relationships

Since water is required for the formation of both the pillow structures and the hyaloclastites, it may be inferred

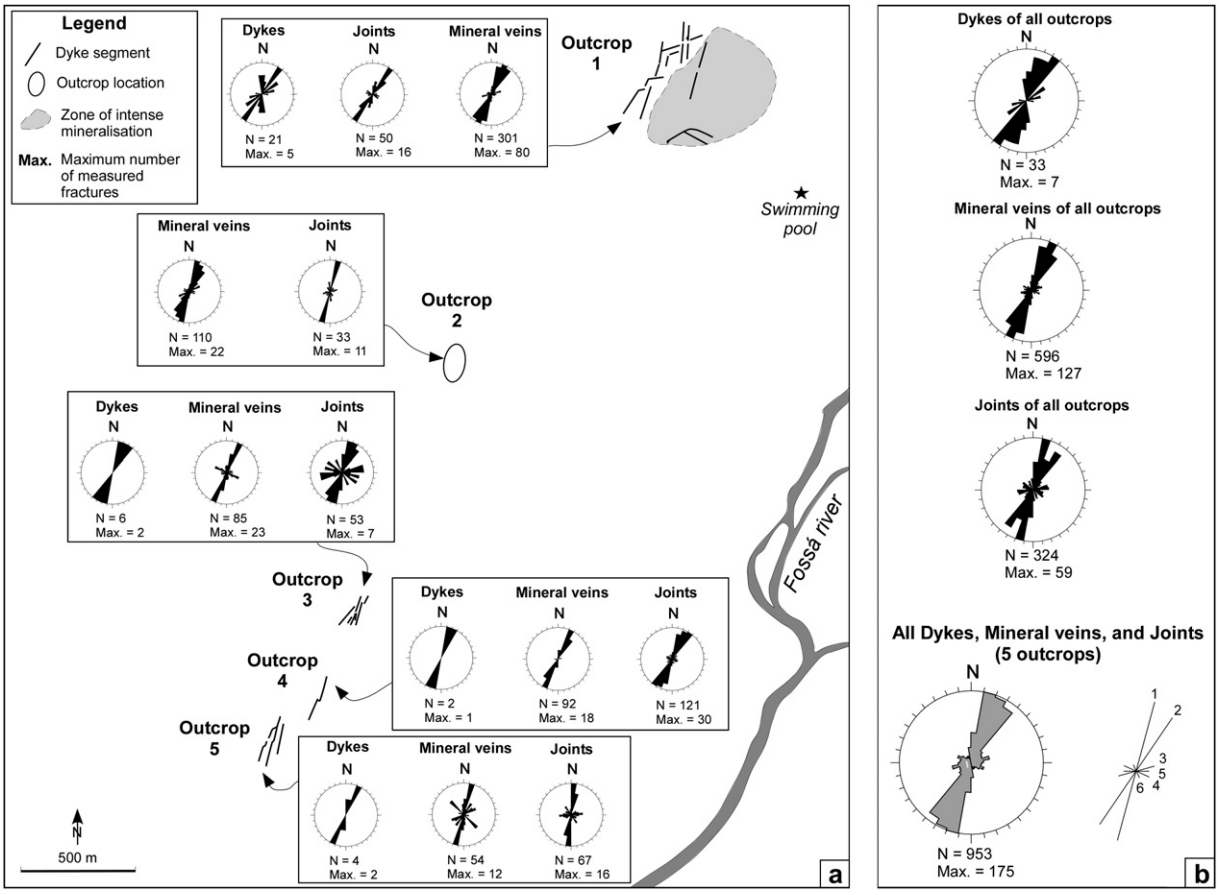

Fig. 4. (a) Map and detailed rose diagrams of mineral veins, dykes, and joints in the five outcrops. (b) Rose diagrams of all mineral veins, all joints, and all dykes, as well as a cumulative rose diagram of all measured fractures. The stick is a simplification of the content of the cumulative rose diagram. Numbers 1 to 6 show the fracture strikes, and the lengths of the lines indicate their frequency as on the adjacent rose diagram. "N" values are the total numbers of measurements, and "Max." values the maximum numbers of measured fractures along the most frequent strike.

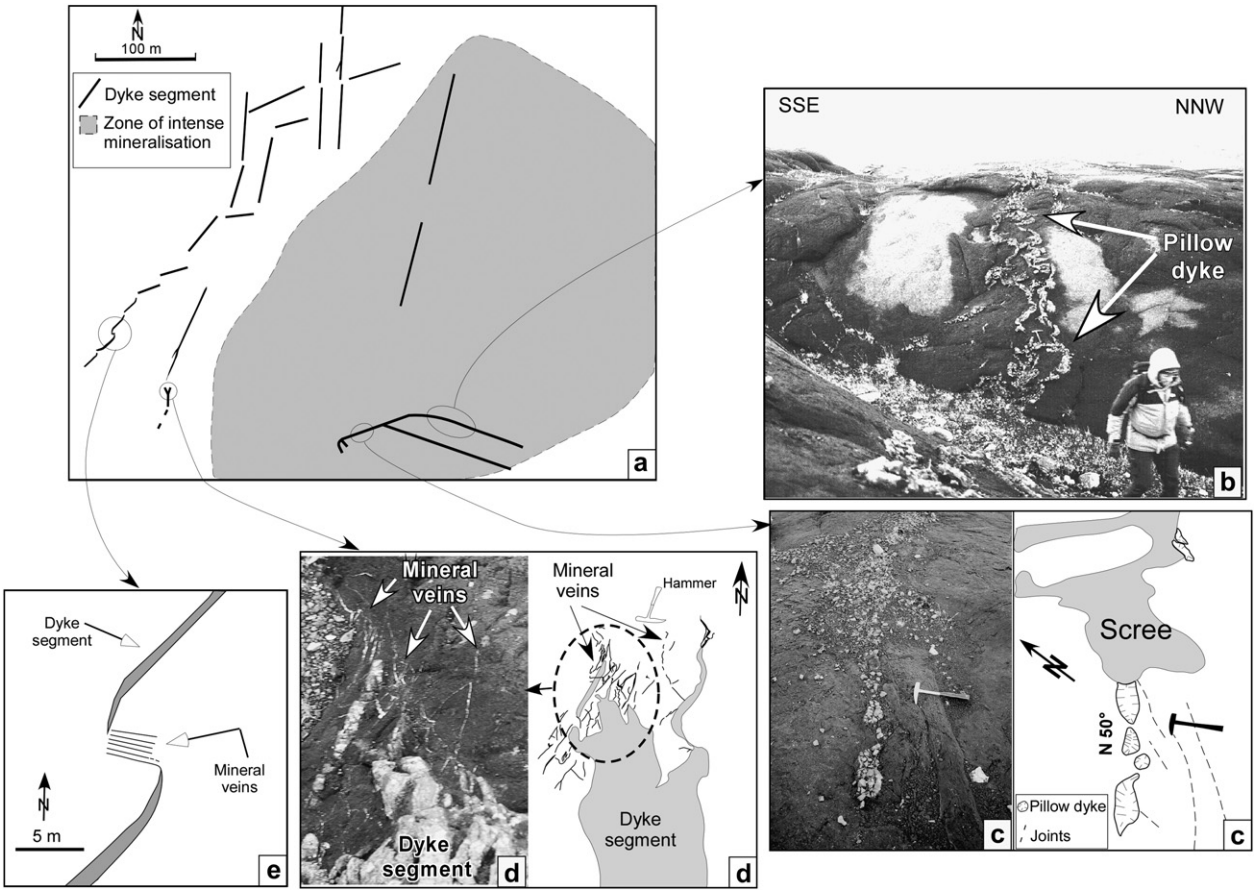

Fig. 5. (a) Detailed map of dyke segments in outcrop 1. (b) Undulating WNW pillow dyke. (c) Portion of the pillow dyke striking NE, parallel to regularly spaced joints. (d) Photo and sketch of mineral veins in a bifurcated dyke tip. (e) Mineral veins perpendicular to two non-overlapping dyke segments in the linkage zone.

that the pillow dyke is contemporaneous with the tuffs and that it injected the hyaloclastites while these were water-saturated and partially consolidated. Thus it is the oldest dyke. It is possible that the pillow dyke intruded tectonic fractures, as do most dykes in the surrounding Hreppar block (Khodayar and Einarsson, 2002b; Khodayar and Franzson, 2004). The observed zeolites indicate a temperature of 50° to 100 °C, implying that the host tuffs were at a burial depth of a few hundred metres when the geothermal system became active. The main phase of mineralisation occurred at this time.

4.1. Phase of main mineral vein formation

4.1.1. Timing of mineral veins

Since most veins do not penetrate adjacent non-pillow dykes, they are interpreted to mostly pre-date the dykes. Consequently, not only is the vein density less in the dykes and the vein themselves diffuse, but the thickness of the veins in the host rock tuffs greatly exceeds the thickness of the veins in the dykes. The rare veins that penetrate the dykes are: (a) veins intruding a bifurcated dyke's tip (Fig. 5d), where most veins strike parallel to the dyke; (b) thin mineral veins forming a linkage between two non-overlapping dyke segments (Fig. 5e); (c) veins with scattered strikes cutting the pillow dyke; and (d) thin remnants of secondary minerals in cooling joints of numerous non-pillow dykes.

4.1.2. Tectonic pattern of mineral veins

The mineral veins strike predominantly NNE with a peak at N21°E–N30°E, but N–S veins with a peak at N10°E–N20°E (Fig. 4b) are also frequent (Figs. 7 and 8). Less common are veins striking ENE, WNW, and E–W with peaks at, respectively, N70°E–N80°E, N110°E–N120°E, and N90°E–N100°E. The NNW veins are the least common, with a peak at N150°E–N160°E (Fig. 4a,b). Examination of 74 intersection relationships show that veins cross-cut or offset each other at different locations, so overall the sets are interpreted to be coeval (Fig. 9).

Strike-slip motion was identified along five sets of veins (Figs. 7–9). The N–S veins (N178°E–N20°E) showed dextral motion based on pull-apart structures in horizontal section (Fig. 7a), or on their left-stepping *en échelon* arrangement (Fig. 8a). In some cases, the horizontal displacement could be measured from the offset of perpendicular or oblique adjacent veins (Fig. 7a). The offset along these N–S veins varies from a minimum of 0.5 cm near the fracture tips, to a maximum of 1.5 cm in the middle part of the mineral veins (Fig. 7a).

A few ENE veins striking N51°E–N80°E indicate sinistral motion. The sense of their motion was deduced from their right-stepping *en échelon* arrangement and in a few cases,

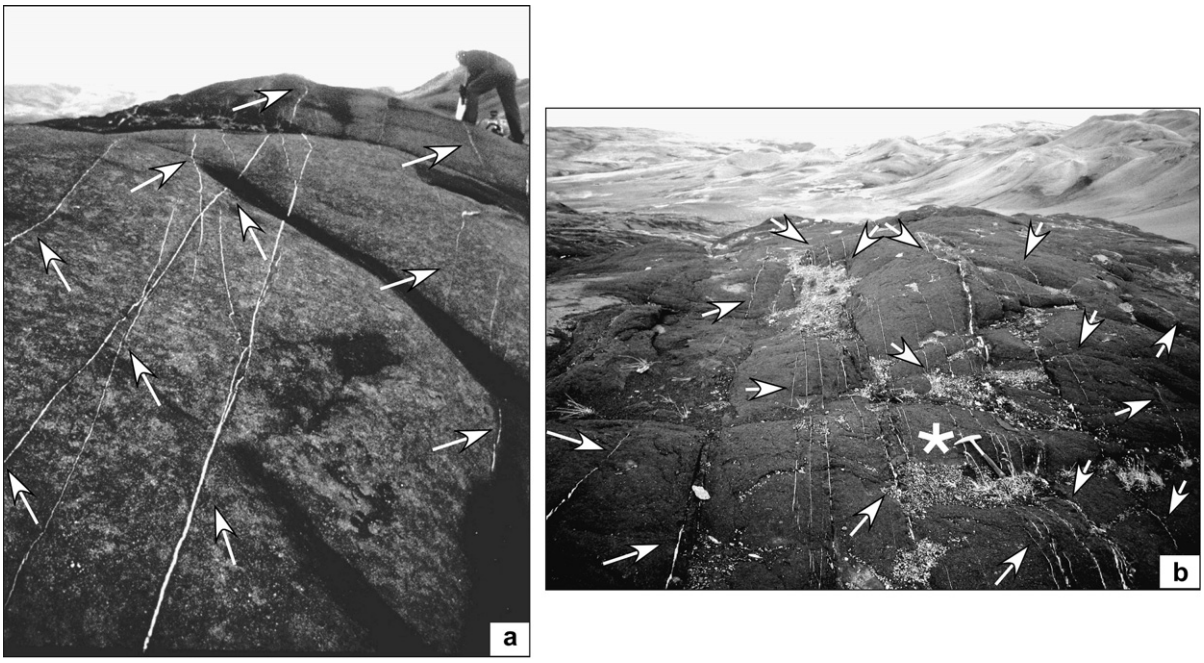

Fig. 6. (a) View to the north along parallel and oblique mineral veins, with a person for scale. (b) View to the NNE along a dense network of mineral veins. The star indicates a hammer for scale. White arrows on both pictures point to veins in the volcanic tuffs.

from the displacement of adjacent perpendicular or oblique veins (Fig. 7b). The N–S and the ENE veins form a conjugate dextral and sinistral strike-slip set, similar to the strike-slip faults of the SISZ. Sinistral motion along E–W (N81°E–N100°E) and WNW (N101°E–N140°E) veins was inferred using criteria such as left-stepping *en échelon* arrangement, displacement of adjacent veins, and pull-apart structures (Fig. 8a,b). In rare cases (Fig. 9), sinistral offset was also identified along NNW veins (N141°E–N170°E).

No strike-slip motion was observed along the NNE veins (N21°E and N50°E). Therefore, we suggest that the NNE veins whose strikes are parallel to the rift zones are purely extensional.

4.1.3. Secondary minerals infilling

In an attempt to establish a relative chronology, we also analysed 11 samples of secondary minerals from outcrop 1 with XRD. Calcite, analcime, thomsonite, scolesite, gyrolite, reyerite, truscotite, hydroxyapophyllite, and clay minerals are found equally in the veins, in the host rock tuffs, and in rare dykes. The minerals indicate deposition at a temperature of 50–100 °C and a burial depth of 500–700 m (Walker, 1960). No significant differences in the mineral assemblage appear between vein strikes, indicating that all six sets were open during the same time interval. Indenting calcite and zeolite crystals observed under a binocular microscope suggest that the veins were open during mineral growth. This implies that veins of all six sets have an extensional component.

4.2. Phase of non-pillow dykes injection

Non-pillow dykes strike predominantly NNE–NE (N30°E–N40°E), but N–S dykes, with a wide strike-range from N171°E to N20°E (Fig. 4a,b) are also common. Less frequent are dykes striking ENE (51°E–60°E and N70°E–N80°E). The E–W dykes (N81°E–N100°E) are the least common (Fig. 4a,b). Dyke cross-cutting relationships, which might have clarified the chronology of dyke injection relative to the strike, were not observed.

Three major sets of dykes striking NNE–NE, N–S, and ENE are interpreted to post-date mineral veins (Fig. 4b). The rift-parallel NNE–NE dykes predominate, and N–S dykes are equally common. The N–S and the ENE veins behave as a conjugate set of dextral and sinistral strike-slip faults. Likewise, field examples from the rift-jump sites of Hreppar (Khodayar and Franzson, 2004), of Borgarfjörður (Khodayar and Einarsson, 2002a), and from the old crust within the SISZ (Khodayar et al., in preparation), confirm dyke injection into N–S dextral and ENE sinistral strike-slip faults.

4.3. Joints

The joints strike predominantly N–S, with a peak at N10°E–N20°E (Fig. 4), but the NNE–NE (N30°E–N40°E) joints are less frequent. Next come the ENE (N70°E–N80°E) and the E–W (N80°E–N90°E) joints, which are equally common (Fig. 4b), followed by the WNW joints (N120°E–N130°E). The NNW set (N150°E–N160°E) is more prominent among joints than among dykes and veins (Fig. 4b). Joints crop out as often near the dykes as the veins. Field evidence do not indicate if the joints were formed in relation to dykes, to veins, to undifferentiated faults in the tuffs, or on their own. A comparison of the three fracture types suggests that the most common joints and dykes show similar strikes, i.e. NNE–NE and N–S.

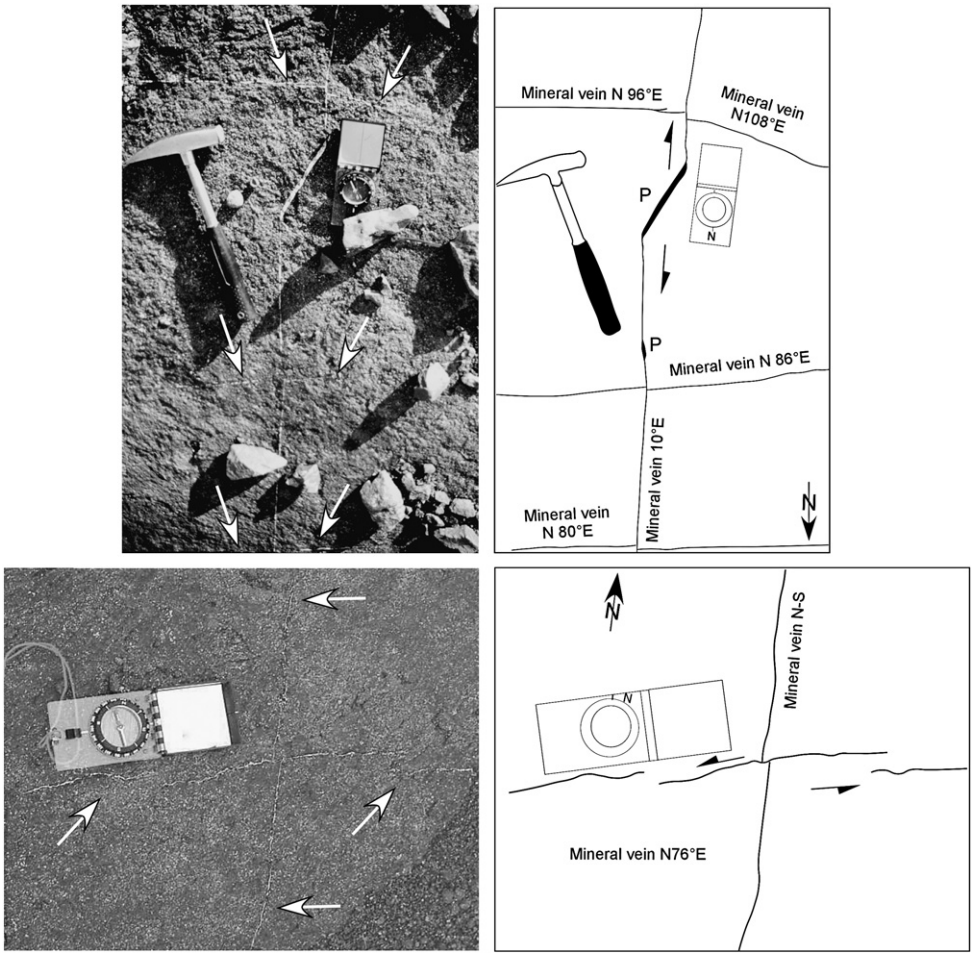

Fig. 7. View map (photograph and sketch) of strike-slips along N–S and ENE veins. (a) A dextral N–S vein displacing E–W and WNW veins. The lateral separation is 1.5 cm in the central part (upper part of the figures), and 0.5 cm towards the tip of the N–S vein. The letter ''P'' indicates a pull-apart structure filled by secondary minerals. (b) Right-stepping *en échelon* sinistral ENE vein displacing a N–S vein.

5. Origin of the Thjórsárdalur fracture pattern

5.1. Fracture pattern of the SISZ

The E–W striking boundaries of the SISZ are not visible on the surface, but the existence of a transform zone with an E–W strike was demonstrated by seismicity (Ward, 1971; Björnsson and Einarsson, 1974). Within the SISZ, seismic activity occurs primarily on N–S dextral strike-slip faults (Figs. 1 and 10a) with a bookshelf mechanism (Einarsson et al., 1981), and secondarily on ENE sinistral strike-slip faults. These faults are by far the most common. They are classically called ''earthquake fractures'' as they are, or have been, seismically active. Detailed mapping of shear fractures in the SISZ shows that six fracture sets are present within the transform zone (Einarsson et al., 2005). A few selected examples of these fractures are shown in Fig. 10b–e. Generally, the N–S dextral segments strike N171°E to N20°E, and the ENE sinistral segments N51°E and N80°E. The NNE–NE segments (N21°E–N50°E) are frequently dilational, with longer segments and wider opening. The E–W segments (in the range N81°E–N100°E) show sinistral motion as well.

Irrespective of strike, the earthquake fractures consist primarily of extensional structures (sink hole and tension gashes) at the surface, and secondarily of compressional features, i.e. push-ups (Fig. 10b–d). Extensional fractures show mostly opening and dilation across segments, and a few normal-slips (Einarsson et al., 2005). The strike-slip behaviour of earthquake faults is mainly inferred from *en échelon* geometry, the right or left-stepping organisation of fault segments (Einarsson and Eiríksson, 1982), and in a few cases from the offsets of markers in the field.

5.2. Fracture pattern of Thjórsárdalur

The fracture pattern of Thjórsárdalur is analogous to the earthquake fracture pattern of the SISZ in terms of strikes, frequencies (Figs. 4b and 10e), and motions: (a) dextral and sinistral motions occur along the conjugate set of N–S (Figs. 7a, 8a, 10e), and ENE fractures (Figs. 7b and 10e); (b) sinistral motion occurs to a lesser extent along the E–W set (Figs. 8a and 10e); and (c) the WNW and the NNW fractures are the least common, with sinistral motion observed only along mineral veins in Thjórsárdalur (Figs. 8b,c and 9).

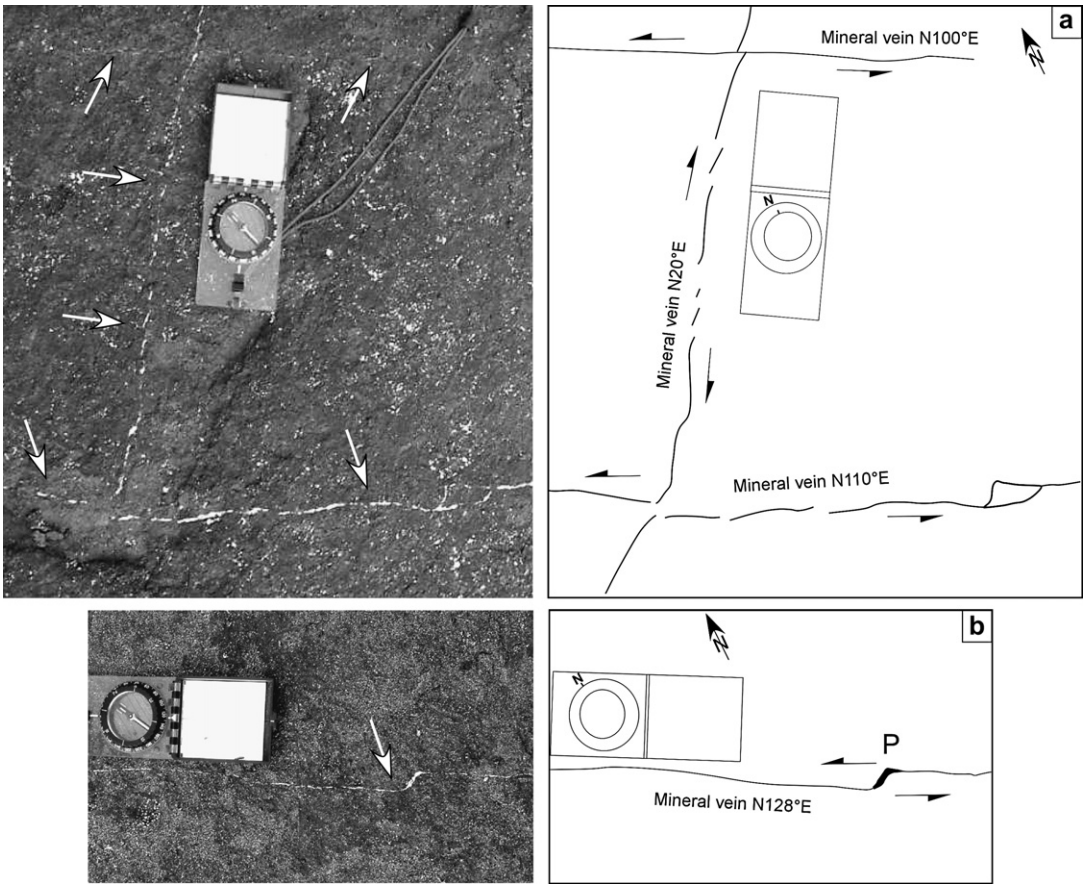

Fig. 8. View map (photograph and sketch) of strike-slips along a N–S vein, an E–W vein, and a right-stepping *en échelon* WNW vein. (a) E–W and WNW sinistral veins displacing a left-stepping N–S vein. The lateral separation is at most 2 cm. (b) Sinistral strike-slip along a WNW vein. The letter "P" indicates a pull-apart structure filled by secondary minerals.

The co-existence of the five sets of shear fractures with the NNE–NE rift-parallel fractures, the cross-cutting mineral veins (Fig. 9), and the similar mineral assemblage in veins of all trends imply the coeval activity of a rift and a transform zone at the latitude of Thjórsárdalur. The influence of the rift zone seems greater than that of the transform zone during the outbreak of mineral veins, as indicated by the greater frequency of the NNE veins (Fig. 4b). But a greater frequency of the N–S (whole set) and ENE dykes reflects a greater influence of the transform zone during the injection of the non-pillow dykes.

5.3. A Riedel shear model for Thjórsárdalur and SISZ

Vialon et al. (1991) presented a new interpretation of the Riedel shear fractures (Riedel, 1929) in a shear zone. They suggest that, under a given NW extension and a NE compression (Fig. 11), an E–W shear zone (similar to SISZ) undergoes sinistral motion, and will consist of at least one system of Riedel shear fractures and one set of extension fractures. But successive orders of fractures, up to four, appear in time within the shear zone as the deformation intensifies: The extensional (T) fractures strike NNE. The (R′) and (R) fractures are, respectively, N–S dextral and ENE sinistral and form an angle of 60°, and may be the most abundant secondary fractures. The (P) fracture is a symmetrical system to (R) and is sinistral. The (Z) and (X) axes are, respectively, the axis of maximum shortening and maximum elongation within the shear zone. Vialon et al. (1991) state that the Riedel fractures are repetitive and spread throughout the entire shear zone, regardless of how many orders of fractures are present. Furthermore, frequently the (R′) or (R) system predominates in the shear zone.

We interpret the data from Thjórsárdalur in the context of the Riedel-related model (Figs. 11 and 12) as follows. (a) The conjugate set of N–S dextral and ENE sinistral earthquake fractures, mineral veins, and possibly dykes act, respectively, as (R′) and (R) shear fractures (Fig. 12b). The WNW striking (P) fractures are present in the SISZ (Fig. 10d–e), and also in Thjórsárdalur where they are sinistral (Fig. 8a,b). The NNE–NE veins, dykes, and possibly some of the joints in Thjórsárdalur (Fig. 4b), as well as the open segments in the SISZ (Fig. 10b–e) behave as (T) fractures. That the frequency of the NNE–NE set is greater in Thjórsárdalur than in the SISZ, however, and that this set is filled with secondary minerals and magma in Thjórsárdalur, indicates that these extension fractures are primarily formed within the rift zone. (b) The N–S (R′) fractures are the most frequent (Figs. 4b, 10e, 11). (c) The shear fractures in Thjórsárdalur and the SISZ crop out over a large area both in the Hreppar block (Khodayar and Einarsson, 2002b; Khodayar and Franzson,

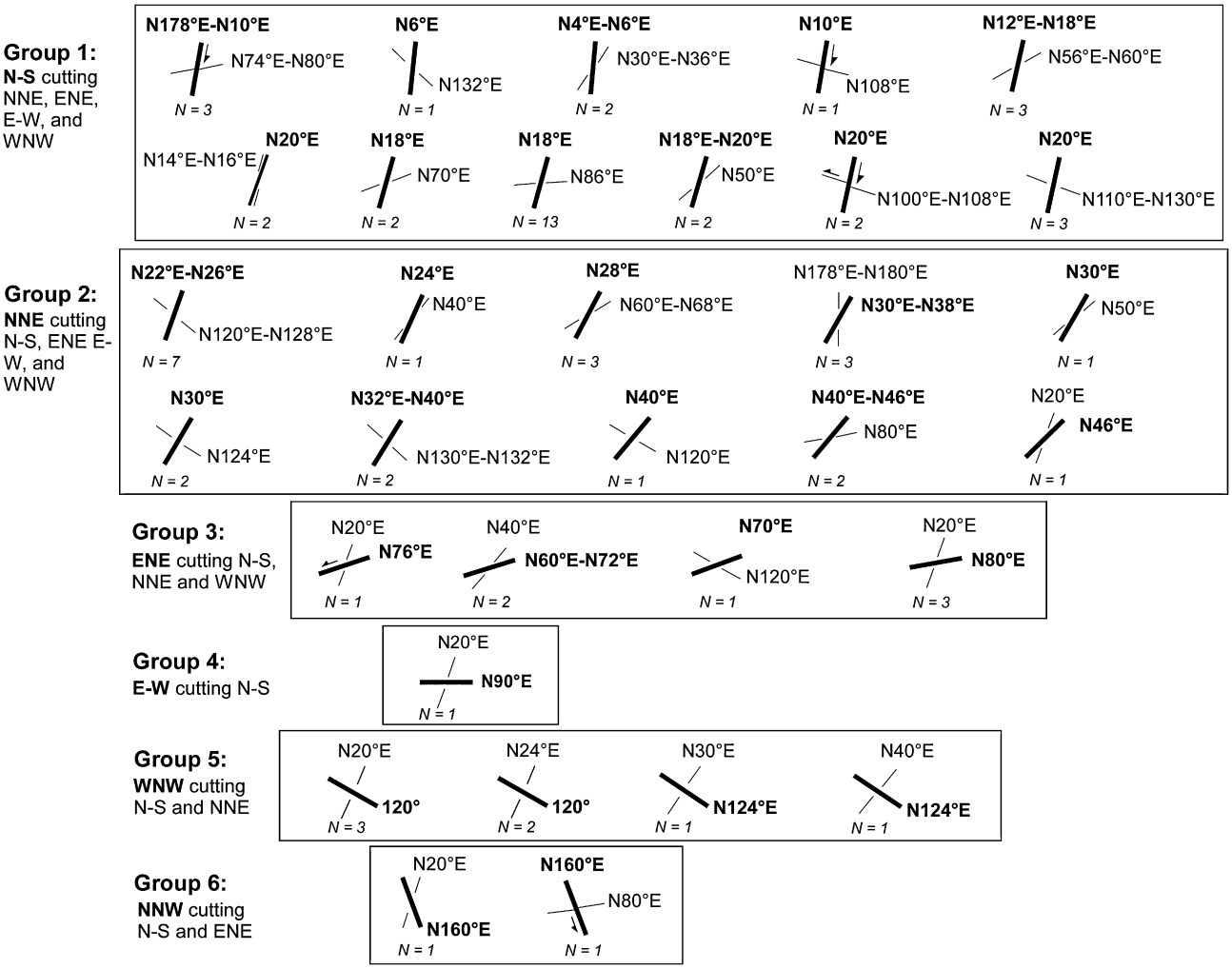

Fig. 9. Vein cross-cutting relationship, mainly from outcrop 1 (thick black line indicates the younger vein in each case). See text for explanation.

2004), and within the active transform zone (Einarsson et al., 2005).

The differences between our model and that of Vialon et al. (1991) are twofold. (a) Two additional shear fractures are present in Thjórsárdalur (Fig. 12a,b) and in the SISZ (Fig. 10b–e). The E–W shear fractures (PS) are parallel to the boundary of the SISZ and act sinistral (Figs. 8a and 10b–e). The NNW (X) shear fractures are the least common in both contexts, and their sinistral motion was identified in Thjórsárdalur (Figs. 9 and 10b–e). The (X) fractures could be a symmetrical system to the (PS) fractures, and the latest set to form within shear zones. (b) The strike-ranges of fracture sets are wider in our model (Fig. 12b) than in the model of Vialon et al. (1991). The reason could be that the observed fracture pattern lies in oceanic crust and not in the continental crust.

5.4. Plate motion, stress field, and strain

Based on the consistency of the Icelandic fracture geometries to the Riedel shear model, we suggest a minimum stress σ_3 between N135°E and N150°E, and a maximum stress σ_1 between N45°E and N60°E at the time of fracture formation in the Thjórsárdalur region (Fig. 12). At present, two rift zones and one transform zone accommodate the displacement south of 65°N in Iceland. As indicated by the average strike of normal faults, extension fractures and eruptive fissures, the RLRZ strikes N30°E and the ERZ N45°E. These strikes are consistent with an extension where σ_3 would be N120°E across the RLRZ and N135°E across the ERZ (Fig. 12c). Thus the same extension could be responsible for the deformation across both the ERZ and the SISZ.

While the NUVEL-1A global plate motion model (DeMets et al., 1990) predicts a widening in the direction N104°E across the Iceland region, it does not account for the presence and the spreading across the micro-plates such as the Hreppar block. The N104°E direction would predict a rift zone striking N14°E. The contemporaneous development of two rifts and a transform zone perturbs the stress field, which would cause variations from the ideal predicted fracture geometries and kinematics. Though reliable recent stress measurements are not available in the Hreppar block, short-term continuous and intermittent GPS measurements have recorded perturbations. These measurements indicate deviation of displacements both across the rift zones and the SISZ compared to the direction

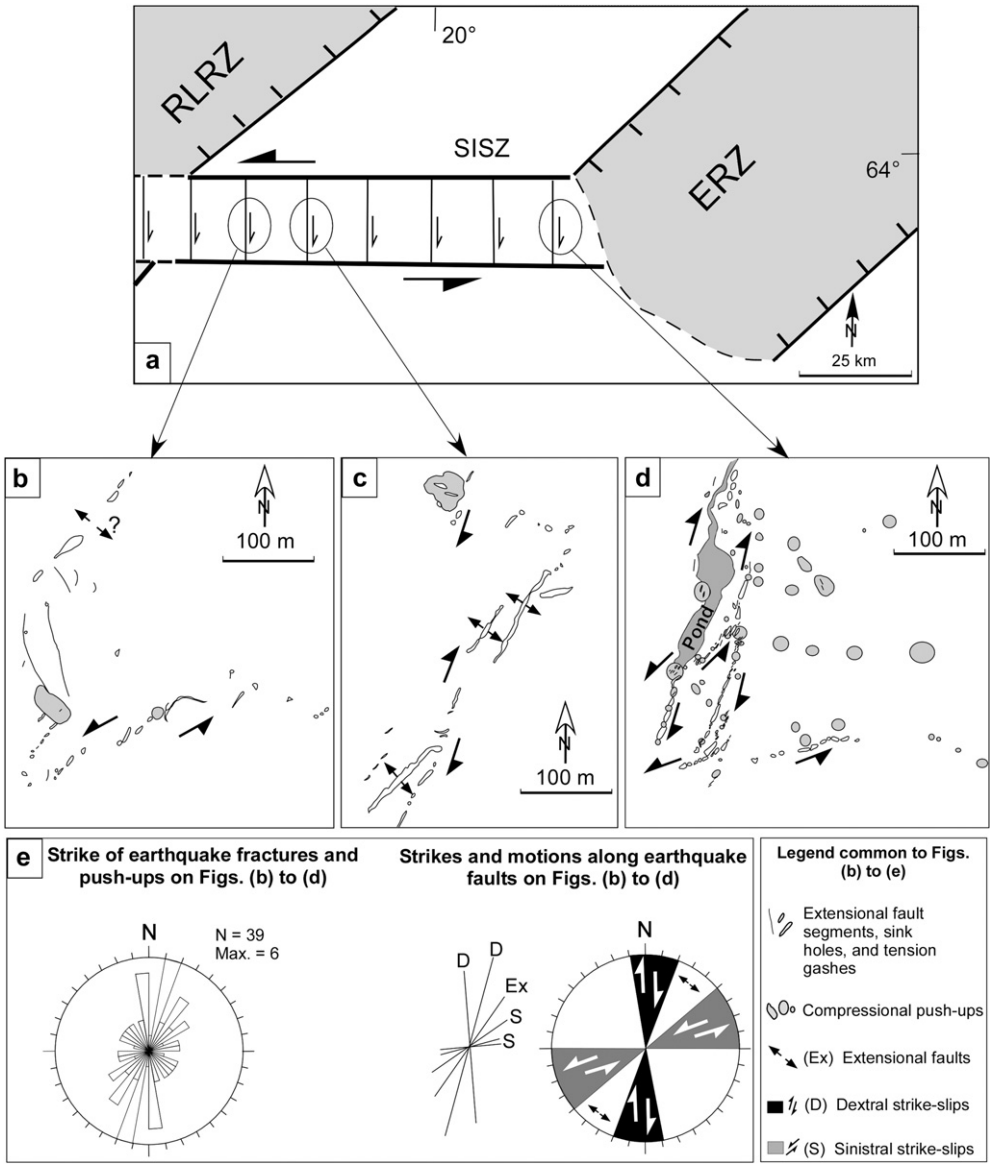

Fig. 10. (a) Map of the Reykjanes-Langjökull Rift Zone (RLRZ), the Eastern Rift Zone (ERZ), and the South Iceland Seismic Zone (SISZ). Only the main earthquake fractures, striking N–S, are shown schematically within the SISZ. Details for: (b) Hraungerði, (c) Austurkot, and (d) Selsund faults. Maps (b) and (c) are after Einarsson et al. (2005), and map (c) after Einarsson et al. (2004). (e) Rose diagram of the strikes of fracture segments and the alignment of push-ups. The stick shows the observed motions along fracture sets, and the three-color rose diagram shows the strike-ranges of fracture types. "N" and "Max." are defined as in Fig. 4.

of absolute plate motion predicted by the NUVEL-1A model (Sigmundsson et al., 1995; Thorbergsson et al., 2002; Geirsson, 2003). For example, a 6-year GPS study in the period 1986–1992 (Sigmundsson et al., 1995) showed a relative displacement of the American plate compared to the Eurasian plate in the direction N117°E ± 11°. This displacement predicts a rift zone striking N27°E.

6. Overview and implications of the results

Our structural analysis in the southern part of the Thjórsárdalur central volcano indicates a six-set fracture pattern. Five sets are shear fractures (Fig. 12a), similar to the shear fractures in the SISZ in terms of strikes, frequency, and motions (Fig. 10b–e). The shear fractures are indicative of a transform zone activity farther north, at the latitude of Thjórsárdalur, and can be explained by a Riedel shear model within a shear zone (Fig. 12b). One set is extensional and predominantly formed within the ERZ where the volcano originated before shifting westward. We base our suggestion of the origin of Thjórsárdalur volcano on its relative young age and short distance from the axis of the ERZ, and on the gentle dip of the volcanic material towards this rift zone. Such regional dips result from the tilt of the volcanic succession towards the active rifts, and are due to accumulation of volcanic material, extension and subsidence along the rift axes (Walker, 1963; Pálmason, 1973).

The six-set fracture pattern is not restricted to Thjórsárdalur but is spread throughout the Hreppar block (Khodayar and Einarsson, 2002b; Khodayar and Franzson, 2004) and also the Borgarfjörður rift-jump block (Khodayar et al., 2004).

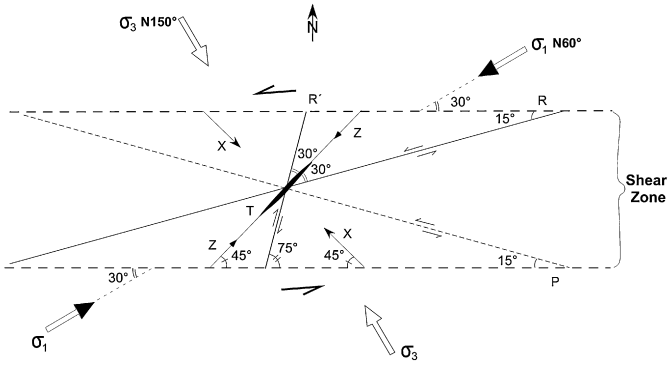

Fig. 11. Riedel shear model after Vialon et al. (1991). See text for explanation.

7. Implications for unstable plate boundaries at spreading centres

Current discussion of unstable plate boundaries is mostly based on examples from fast spreading ridges. These studies indicate a strong relation between the propagating/receding rifts and the migrating transform zone with four main features: the "V" shape structures, with zones of inner and outer pseudo-faults (Hey et al., 1980); fracture rotation from parallel to the rift to oblique to the transform zone (Phipps Morgan and Kleinrock, 1991); reverse faults resulting from compression by shortening (Phipps Morgan and Kleinrock, 1991); and book-shelf tectonics within the transform zone (Kleinrock and Hey, 1989; Phipps Morgan and Kleinrock, 1991). Present data on slow-spreading ridges do not allow the modelling of all aspects of rift-jumps and migrating transform zones. Nevertheless, three basic observations can be made in South Iceland that have implications for slow-spreading unstable plate boundaries.

(1) The transform zone of the SISZ is 20–30 km wide and some 80 km long, with typical shear fractures. Such fractures are also observed in the Thjórsárdalur volcano and throughout the Hreppar rift-jump block (Khodayar and Einarsson, 2002b; Khodayar and Franzson, 2004). We interpret the existence of a typical transform-zone fracture pattern far away from the present location of the zone implies to mean that the transform zone itself must have migrated southward by a distance corresponding to the current width of the SISZ (Fig. 13a,b) while Thjórsárdalur was forming in the ERZ and shifting away from this rift zone.

(2) Since a transform zone connects two segments of active rifts, the southward migration of the SISZ raises two questions:

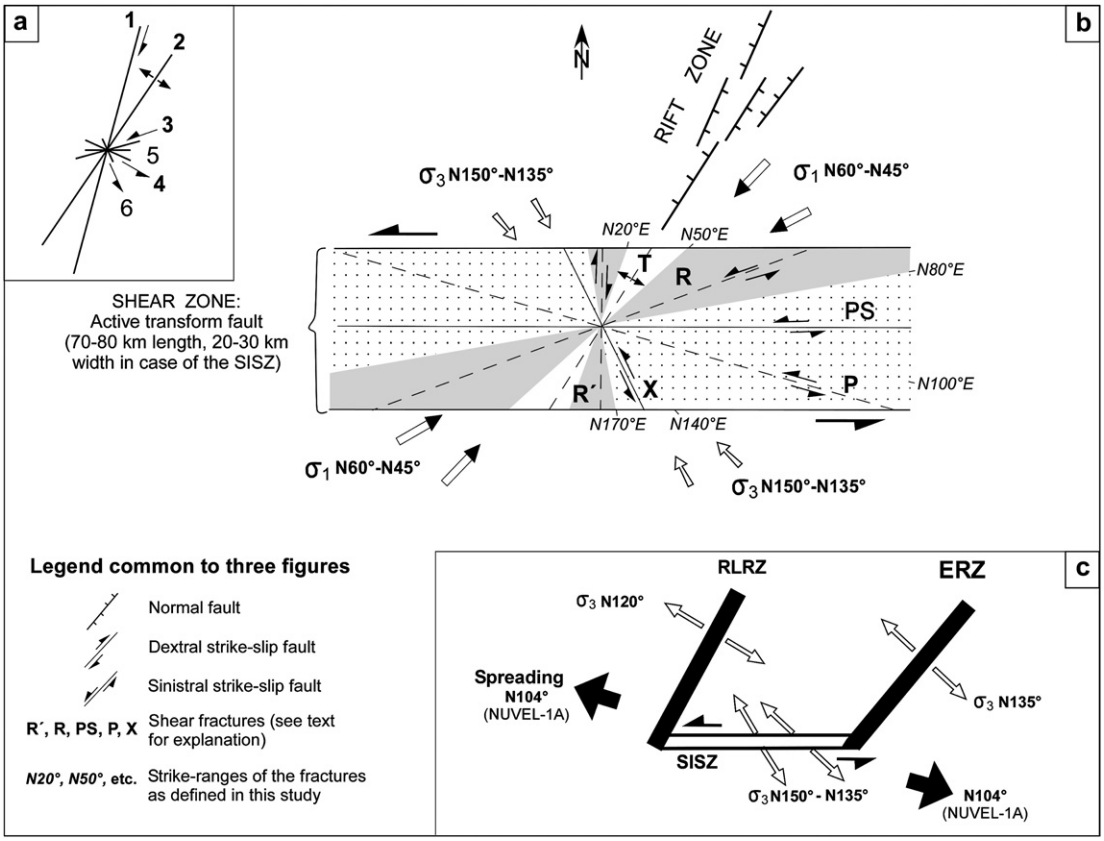

Fig. 12. (a) The six fracture geometries and their motions in Thjórsárdalur. (b) Interpretation relating the fracture sets to Riedel fracture model. During contemporaneous rift and transform activity the shear fractures are generated within the E–W Riedel shear zone, while the extension fractures of the rift zone, presented schematically, are produced outside the shear zone. The dashed lines show modes of shear. The background pattern and the corresponding values in italics show the strike-ranges of the six fracture sets (grey is for dextral Riedel shears, dots for sinistral Riedel shears, and white for extensional fractures). (c) Schematic figure of the directions of spreading plates, and extension across Reykjanes-Langjökull Rift Zone (RLRZ) and Eastern Rift Zone (ERZ). The strikes of the rift zones are deduced from the average strikes of fissure swarms taken from Jóhannesson and Sæmundsson (1998). The directions of extension across the South Iceland Seismic Zone (SISZ) are taken from (b).

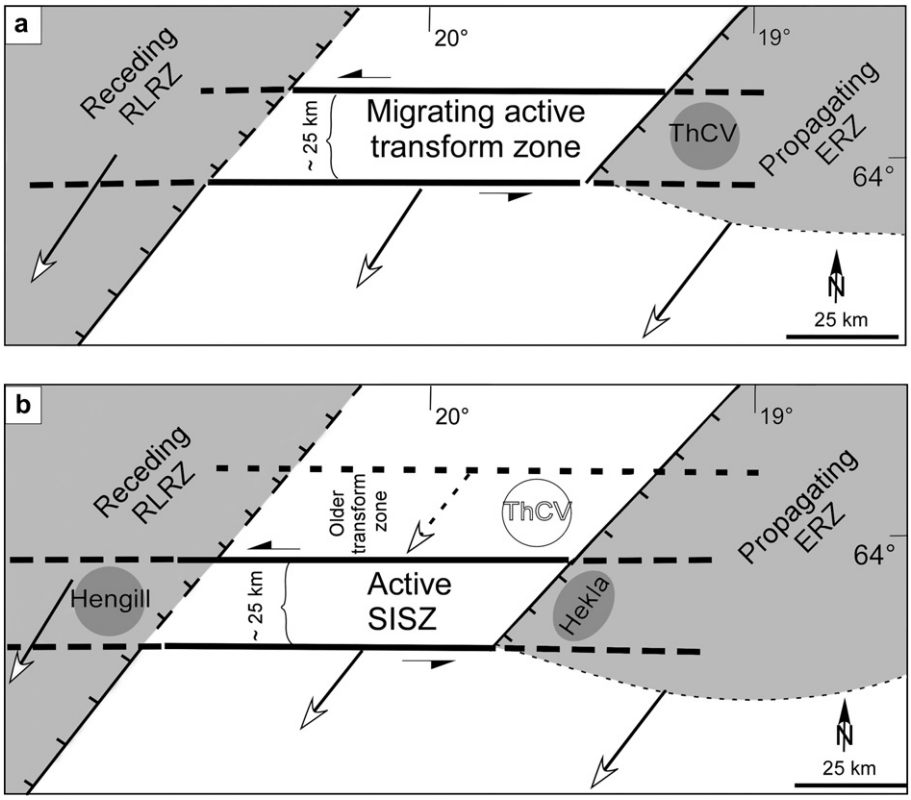

Fig. 13. (a) Schematic sketch showing the initial position of the Thjórsárdalur central volcano (ThCV) at the plate boundary. (b) Position of the volcano after it shifted away from the rift zone, and after the transform zone migrated southward by a distance equivalent to the current width of the SISZ. The dashed white arrows indicate the direction of propagation of the ERZ, the recession of the RLRZ, and the migration of the active transform zone.

(a) Is the RLRZ receding and is the ERZ propagating? Data on various time scales support this interpretation. The rate of spreading in Iceland is roughly 2 cm/yr. Theoretically, this rate should be the sum of the activity of the RLRZ and that of the ERZ if both segments were equally active. GPS measurements in 1986–1992 show that the RLRZ accommodates about 15 ± 15% of the plate motion and the ERZ about 85 ± 15% (Sigmundsson et al., 1995). On a longer time-scale, the volume of lavas $\geq$1 km^3 (Hjartarson, 2003) demonstrates that the ERZ has been more active than the RLRZ over the last 15,000 yr. Magnetic data indicate that also on a million-year scale, the RLRZ has been less active than the ERZ in accommodating the total crustal spreading (Jónsson et al., 1991). The weight of evidence thus points to the ERZ as being more active than the RLRZ. We infer the direction of extension in the study area to be between N135°E and N150°E, which is closer to that across the ERZ than the RLRZ (Fig. 12b,c). Such extension is also consistent with both the SISZ and an older E–W shear zone at the latitude of Thjórsárdalur, which we interpret to mean that the southward migration of the transform zone is closely related to the propagation of the ERZ in the same direction (Figs. 12 and 13).

(b) Are the structural models of unstable rift zones and transform faults at fast-spreading ridges applicable to Iceland? In South Iceland, the magnetic pattern shows neither a "V" shape nor an inner or outer zone of pseudo faults in the Hreppar block (Jónsson et al., 1991). The rotation of the fractures is either not noticeable (Jóhannesson and Sæmundsson, 1998; Khodayar and Einarsson, 2002b; Khodayar and Franzson, 2004), or insignificant (Sigmundsson et al., 1995) in the Hreppar block, and reverse faults resulting from compression by shortening are absent (Khodayar and Einarsson, 2004). Bookshelf tectonics, however, is an integral part of deformation in the SISZ (Sigmundsson et al., 1995).

(3) Thjórsárdalur is not the only central volcano in Iceland evolving under the coeval activity of rift and transform fault zones. South of 65°N, two volcanoes, Hekla and Hengill, are located at the ends of the SISZ (Fig. 2a). Hengill, at the western end of the SISZ, is the southernmost central volcano in the RLRZ before the plate boundary changes to oblique rifting on the Reykjanes Peninsula (Figs. 1 and 2a). This volcano has been the subject of intensive study because of its geothermal development. Despite the presence of non-parallel rift fractures in Hengill (Sæmundsson and Friðleifsson, 2003), the fracture pattern of the volcano has long been considered as typical of a rift zone only (Jóhannesson and Sæmundsson, 1998). Analysis of fault plane solutions of earthquakes in 1998 revealed that at least the N–S, NE, and ENE fractures are active at a depth of 1–8 km (Árnason and Magnússon, 2001). Thus, three of the six fracture sets discussed in our study area are active at Hengill. Our observations of fractures in Hengill from aerial photographs indicate that all the six fracture sets from the study area crop out at the surface

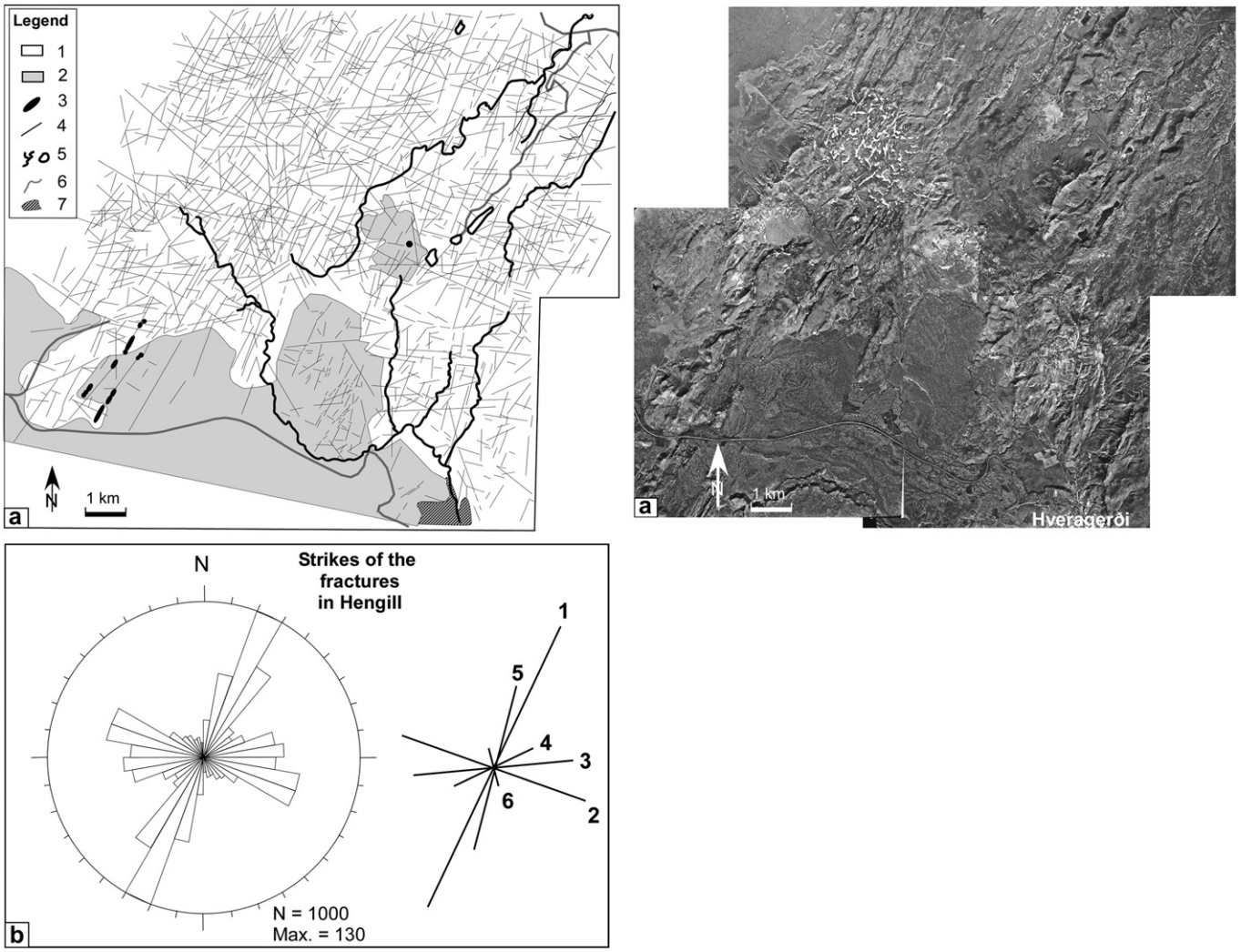

Fig. 14. (a) Sketch in map view and aerial photographs (© *Landmælingar Íslands, licence L05070008*) of the Hengill area. (b) Rose diagram of the strike of the fractures observed on aerial photographs in the Hengill area. The stick is a simplification of the adjacent rose diagram, and the numbers show the order of the most frequent fracture sets. Legend for the sketch: 1. Lavas, hyaloclastites, sediments 10,000 yr–0.7 m.y.; 2. Postglacial lavas younger than 10,000 yr; 3. Some eruptive sites; 4. Undifferentiated fractures; 5. Lakes and rivers; 6. Roads; 7. Town of Hveragerði. "N" and "Max." are defined as in Fig. 4.

(Fig. 14a,b), albeit with a slightly different frequency, possibly because Hengill is at an earlier stage in its evolution.

In summary, the analysis of the Thjórsárdalur region supports an interpretation that the SISZ has migrated southward with propagation of the ERZ. This migration of synchronous transform and rift systems at a slow-spreading centre yields a distinctive pattern of secondary faults, dykes, veins and joints, but lacks some of the elements found at similar migration sites for fast-spreading centres.

Acknowledgements

Our special thanks go to William Dunne, the editor, for taking the time to improve our paper with his pertinent comments. We are grateful to Sveinbjörn Björnsson for his recommendations. Páll Einarsson kindly made constructive suggestions. Thanks also to Simon Kattenhorn, Stephen Martel, David A. Ferrill (editor), and Amy Clifton for their remarks on an earlier version of our manuscript. This work was supported by the National Energy Authority of Iceland (Orkustofnun), the National Power Company (Landsvirkjun), and Reykjavík Energy (Orkuveita Reykjavíkur).

References

Aronson, J.L., Sæmundsson, K., 1975. Relatively old basalts from structurally high areas in central Iceland. Earth and Planetary Science Letters 28, 83–97.

Árnason K., Magnússon, I. Th., 2001. Geothermal activity in Hengill and Hellisheiði. Results from resistivity survey. Orkustonfun report (in Icelandic), OS-2001/091, 250 p.

Björnsson, S., Einarsson, P., 1974. Seismicity of Iceland. In: Kristjansson, L. (Ed.), Geodynamics of Iceland and the North Atlantic Area. Nato Advanced Study Series. D. Reidel Publ. Comp., Dordrecht, Holland, pp. 225–239.

DeMets, C., Gordon, R.G., Argus, D.F., Stein, S., 1990. Current plate motions. Geophysical Journal International 101, 425–478.

Einarsson, P., 1991. Earthquakes and present-day tectonism in Iceland. Tectonophysics 189, 261–279.

Einarsson, P., Eiríksson, J., 1982. Earthquake fractures in the district Land and Rangárvellir in the South Iceland Seismic Zone. Jökull 32, 113–120.

Einarsson, P., Björnsson, S., Foulger, G., Stefánsson, R., Skaftadóttir, Th., 1981. Seismicity pattern in the South Iceland seismic zone. In: Simpson, D., Richards, P.G. (Eds.), Earthquake Prediction: An International Review. Maurice Ewing Ser, vol. 4. AGU, Washington, DC, pp. 141–151.

Einarsson, P., Khodayar, M., Thorbjarnason, S., the students of Tectonics and Current Crustal Movements in the Faculty of Science, University of Iceland, 2004. Surface ruptures in the South Iceland earthquake of 1912, in: The 2004 Spring Meeting of the Icelandic Geoscience Society, Reykjavík, p. 47.

Einarsson, P., Khodayar, M., Clifton, A., Ófeigsson, B., Thorbjarnarson, S., Einarsson, B., Hjartardóttir, Á.R., 2005. A map of Holocene fault structures in the South Iceland Seismic Zone. Poster at the General Assembly of the European Geosciences Union, Vienna, April, 2005. Abstract EGU05-A-08858.

Friðleifsson, I.B., Haraldsson, G.I., Georgsson, L.S., Gunnlaugsson, E., Björnsson, B.J., 1980. Geothermal survey in Gnúpverjahreppur district. Orkustofnun report (in Icelandic) OS80010/JHD06, 136 pp.

Geirsson, H., 2003. Continuous GPS measurements in Iceland 1999-2002. M.S. thesis, Report VÍ-03014-JA01, Icelandic Meteorological Office, Reykjavík, 94 pp.

Helgason, J., 1984. Frequent shifts of the volcanic zone in Iceland. Geology 12, 212–216.

Hey, R.N., Duennebier, F.K., Morgan, W.J., 1980. Propagating rifts on mid-ocean ridges. Journal of Geophysical Research 85, 3647–3658.

Hjartarson, Á, 1988. The great Thjórsá lava, the largest postglacial lava of the Earth. Náttúrufræðingurinn 58 (1), 1–16.

Hjartarson, Á., 2003. The Skagafjörður unconformity north Iceland and its geological history. PhD. Thesis, Geological Museum University of Copenhagen, 140 pp.

Jancin, M., Young, K.D., Voight, B., Aronson, J.L., Sæmundsson, K., 1985. Stratigraphy and K/Ar ages across the west flank of the northeast Iceland axial rift zone, in relation to the 7 Ma volcano-tectonic reorganisation of Iceland. Journal of Geophysical Research 90, 9961–9985.

Jóhannesson, H., 1980. Evolution of the rift zones in western Iceland (in Icelandic with English summary). Náttúrufræðingurinn 50, 13–31.

Jóhannesson, H., Sæmundsson, K., 1998. Geological map of Iceland, first edition. In: Scale 1:500.000. Tectonics. Icelandic Institute of Natural History, Reykjavík.

Jónsson, G., Kristjánsson, L., Sverrisson, M., 1991. Magnetic surveys of Iceland. Tectonophysics 189, 229–247.

Kattenhorn, S.A., Watkeys, M.K., 1995. Blunt-ended dyke segments. Journal of Structural Geology 17 (11), 1535–1542.

Khodayar, M., Einarsson, P., 2002a. Strike-slip faulting, normal faulting and lateral dyke injections along a single fault: Field example of the Gljúfurá fault near a Tertiary oblique rift/transform zone, Borgarfjörður, W-Iceland. Journal of Geophysical Research 107 (B5), doi:10.1029/2001JB000150. ETG 5, 1–18.

Khodayar, M., Einarsson, P., 2002b. Structural analysis of the Núpur area, Gnúpverjahreppur, South Iceland. Science Institute, University of Iceland report RH-08-2002 and the National Power Company of Iceland Landsvirkjun report, LV-2002/101, 16 pp.

Khodayar, M., Einarsson, P., 2004. Reverse-slip structures at oceanic diverging plate boundaries and their kinematic origin: Data from Tertiary crust of West and South Iceland. Journal of Structural Geology 26, 1045–1960.

Khodayar, M., Franzson, H., 2004. Stratigraphy and tectonics of eastern Núpur/Western Hagafjall in Gnúppverjahreppur, South Iceland. Iceland Geosurvey report, ÍSOR-2004/017, 42 pp.

Khodayar, M., Franzson, F., Björnson, S., Víkingsson, S., Jónsdóttir, G.S., 2004. Tectonic lineaments of Borgarfjörður-Hvalfjörður from aerial photographs, West Iceland, Preliminary results. Iceland Geosurvey report, ÍSOR-2004/021, 47 pp.

Khodayar, M., Franzson, F., Einarsson, P., Björnson, S., in preparation. Geological synthesis of Núpur-Hagafjall-Skarðsfjall, South Iceland: Bedrock and Tectonics. Iceland Geosurvey Report.

Kleinrock, M.C., Hey, R.N., 1989. Migrating transform zone and lithospheric transfer at the Galapagos 95.5°W propagator. Journal of Geophysical Research 94, 13859–13878.

Kristjánsson, L., Jónsson, G., 1998. Aeromagnetic results and the presence of an extinct rift zone in Western Iceland. Journal of Geodynamics 25, 99–108.

Kristjánsson, L., Duncan, R.A., Guðmundsson, Á, 1998. Stratigraphy, paleomagnetism and age of volcanics in the upper regions of Thjórsárdalur valley, central Southern Iceland. BOREAS 27, 1–13.

Pálmason, G., 1973. Kinematics and heat flow in a volcanic rift zone with application to Iceland. Geophysical Journal of the Royal Astronomical Society 33, 451–481.

Phipps Morgan, J., Kleinrock, M.C., 1991. Transform migration: Implication of bookshelf faulting at oceanic and Icelandic propagating ridges. Tectonics 10 (5), 920–935.

Riedel, W., 1929: Zur Mechanik geologischer Brucherscheinungen. Zentralblatt für Mineralogie, Geologie, und Paleontologie, B, 354–368.

Shih, J., Molnar, P., 1975. Analysis and implication of the sequence of ridge jumps that eliminated the surveyor transform fault. Journal of Geophysical Research 80 (35), 4815–4822.

Sigmundsson, F., Einarsson, P., Bilham, R., Sturkell, E., 1995. Rift-transform kinematics in south Iceland: Deformation from Global Positioning System measurements, 1986 to 1992. Journal of Geophysical Research 100 (B4), 6235–6248.

Sigurðsson, H., 1970. Structural origin and plate tectonics of the Snæfellsnes Volcanic Zone, Western Iceland. Earth and Planetary Science Letters 10, 129–135.

Sæmundsson, K., 1970. Interglacial lava flows in the lowlands of Southern Iceland and the problem of two-tiered Columnar jointing. Jökull 20, 62–77.

Sæmundsson, K., 1978. Fissure swarms and central volcanoes of the neovolcanic zones of Iceland, in: Bowes, D.R., Leake, B.E. (Eds.), Geological Journal, 10, 415–432 (Special Issue).

Sæmundsson, K., Friðleifsson, G.Ó., 2003. Geology and geothermal map of Hengill area: Revision of area south of Hengill. Iceland Geosurvey report (in Icelandic), ÍSOR-2003/020, 42 pp.

Thorbergsson, G., Erlingsson, J.S., Rennen, M., Theodórsson, T., Sigurðsson, Th., Jónsson, Ö., 2002. GPS survey in southern Iceland to connect the old triangulation networks to the new geodetic datum ISN93. Orkustofnun report (in Icelandic), OS-2002/010, 53 pp.

Vialon, P., Ruhland, M., Grolier, J., 1991. Éléments de tectonique analytique, second ed. Masson, Paris, 118 pp.

Vilmundardóttir, E.G., Guðmundsson, A., Snorrason, S.P., 1983. Map of bedrock geology Búrfell-Langalda 3540B, 1:50.000 (in Icelandic). Orkustofnun and Landsvirkjun Publishers.

Walker, G.P.L., 1960. Zeolite zones and dyke distribution in relation to the structures of basalts in eastern Iceland. Journal of Geology 68, 515–528.

Walker, G.P.L., 1963. The Breiddalur central volcano, eastern Iceland. Quaternary Journal of the Geological Society of London 119, 29–63.

Ward, P.L., 1971. New interpretation of the geology of Iceland. Geological Society of America Bulletin 82, 2991–3012.